ISSN 0016-7029, Geochemistry International, 2015, Vol. 53, No. 2, pp. 113–132. © Pleiades Publishing, Ltd., 2015.
Original Russian Text © V.B. Naumov, V.A. Dorofeeva, O.F. Mironova, 2015, published in Geokhimiya, 2015, No. 2, pp. 123–143.

Physicochemical Parameters of Formation of Hydrothermal Deposits: Evidence from Fluid Inclusions. III. Uranium Deposits

V. B. Naumov, V. A. Dorofeeva, and O. F. Mironova

Vernadsky Institute of Geochemistry and Analytical Chemistry, Russian Academy of Sciences, ul. Kosygina 19, Moscow, 119991 Russia

e-mail: naumov@geokhi.ru

Received June 26, 2013; in final form, October 31, 2013

Abstract—An original database, which was compiled by the authors, is continuously updated, and now contains data from more than 19 800 publications on fluid and melt inclusions in minerals, was utilized to review and synthesize data on the physicochemical parameters at which hydrothermal uranium deposits and occurrences were formed. The parameters discussed below are temperature, pressure, density, salinity, gas composition of the fluid, and U concentration in the hydrothermal fluid. The database contains data of fluid inclusions in minerals from 90 U deposits and occurrences worldwide. Histograms of the homogenization temperatures of fluid inclusions are presented for such typical minerals of these deposits and occurrences as quartz, calcite, and fluorite. The temperature range most favorable for the origin of U deposits is 100–200°C (67% of the 937 measured temperature values fall within this range), which makes U deposits remarkably different from higher temperature Au–Ag, W, and Sn deposits. These deposits also differ in the salinity of the fluids. The range of fluid salinity of 10–30 wt % equiv. NaCl includes 42% of fluid salinity values measured at U deposits (our database includes 937 measured values), 27% for Au–Ag deposits (10 237 measured values), 27% for W deposits (2333 measured values), and for Sn deposits (1981 measured values). The relatively low temperature of U-bearing fluids and their high salinity testify that these solutions had a high density: 94% of all measured values lie within the range of 0.8–1.2 g/cm^3. Fluid pressure at U deposits broadly varied from 2500 to 300 bar and perhaps even lower values. Data on the chemical composition of the gas phase of the fluid inclusions show a significant diversity of the fluids contained in the inclusions. In certain instances, H_2O–CO_2 fluids give way to fluids rich in CH_4 and N_2 with minor amounts of hydrocarbons. Data are reported on the gas composition of fluid inclusions in the nuclear-reactor zone at three Precambrian U deposits. Analyses of individual inclusions were utilized to evaluate U concentrations in magmatic melts and mineral-forming fluids. The geometric mean U concentration in silicate melts of composition ranging from ultramafic to silicic is 0.92 ppm (8053 measured values), and the analogous values for the fluids is 1.21 ppm (271 measured values).

Keywords: uranium deposits, fluid inclusions, physicochemical parameters

DOI: 10.1134/S0016702914120064

INTRODUCTION

In our earlier publication [1], we have utilized our database (which contained then data compiled from more than 17 500 publications on fluid and melt inclusions) to summarize evaluation of principal physicochemical parameters of natural mineral-forming fluids: their temperature, pressure, density, salinity of the aqueous solutions, and the gas composition of fluids. Fluids involved in magmatic, metamorphic, hydrothermal, and sedimentary processes exhibit broad ranges of their temperature (20–1300°C) and pressures (1–21 000 bar). We have calculated the frequency of occurrence of temperature and salinity values of hydrothermal fluids at 20–1000°C and negative-80 wt % equiv. NaCl and the temperature and density values of these fluids within the ranges of 20–1000°C and 0.01–1.90 g/cm^3. The average composition of the gas phase of natural fluids was evaluated based on more than 3000 individual analyses of inclusions (analyzed by Raman spectroscopy, a technique conventionally most commonly applied to analyze fluid inclusions).

The task of our later study was to synthesize data on the major physicochemical parameters of mineral-forming fluids that were involved in the generation of hydrothermal deposits of various elements (Au, Ag, Sn, W, Mo, Be, Cu, Zn, Pb, Sb, Co, Ni, As, Ba, U, and Hg and deposits of fluorite and Iceland spar. These reviews were made based on our database on fluid and melt inclusions in minerals, which was compiled in 1964 and was continuously updated afterward. The principle of database updating is described in detail in [1, 2]. Physicochemical parameters of fluids at deposits and occurrences of Sn and W [3] and Au, Ag, Pb, and Zn [4] minerals were discussed in our later publications on the basis of data from the database (which then comprised information borrowed from more than 18 500 publications). In addition to temperatures, pressures, salinity, and density of fluid, the aforementioned papers pre-

Table 1. Number of publications (by year) on the physicochemical parameters of natural fluids determined by studying inclusions in minerals from U deposits

Period of time	Number of publications	Number of measured values			
		temperature	pressure	salinity	gas composition
1950–1959	1	1	–	–	–
1960–1969	4	188	13	5	19
1970–1979	16	134	6	60	1
1980–1989	15	55	3	47	29
1990–1999	10	209	–	193	23
2000–2012	26	651	10	636	58
1950–2012	72	1238	32	941	130

sented data on the concentrations of these elements in magmatic silicate melts and mineral-forming fluids.

This paper is a review of currently available information (borrowed from more than 70 publications) on the principal physicochemical parameters of natural fluids that have produced U deposits. This summary includes our extensive original data on fluid inclusions in minerals from U deposits. We have studied 227 samples from 20 U deposits. Some of these data have been reported in our first review (published in 1969) of the temperatures and pressures at which hydrothermal U deposits are formed [5]. Note that herein we discuss only the general characteristics of fluids at U deposits, regardless of their affiliation with certain types of ore associations distinguished by geologists. For example, several classifications of U deposits were suggested based on various features of these deposits employed as criteria in corresponding systematics. We do not touch upon any issues concerning the sources of U, its speciation and circumstances of its transport, and the reasons for and mechanisms of ore deposition.

The representativeness of the information on U deposits is reflected in Table 1. In the course of our research, we have obtained more than 1200 temperature values of mineral-forming fluids, only 32 values of their pressure, 941 values of their salinity, and 130 analyses of the gas composition of the fluids. Our original data make up 17% of all measured values of fluid temperatures, 56% of the pressure values, 3% of the salinity values, and 17% of the gas compositions. Physicochemical parameters of fluids were determined at 90 U deposits and occurrences worldwide. It can be seen that studies of parameters of mineral-forming fluids were launched as late as the 1960s, and U deposits were most intensely studied in the 21st century.

Table 2 summarizes (in chronological order) all available literature data on the ranges of physicochemical parameters (temperature, pressure, and salinity) of fluids at U deposits and occurrences derived from data on fluid inclusions. Our original data on these parameters are presented in Table 3 (in which the minerals in which fluid inclusion were studied and the numbers of measurements are also specified). Below we successfully discuss data obtained by various researchers on certain parameters of mineral-forming fluids at U deposits.

TEMPERATURE OF MINERAL-FORMING FLUIDS

Minerals from U deposits most commonly contain two-phase gas–liquid inclusions. When heated, they homogenize into liquid at temperatures below 300°C, which suggests that the inclusions contain relatively dense aqueous solutions. Figures 1 and 2 display micrographs of such inclusions at room temperature in various minerals. At certain deposits (for example, Zhel-

Fig. 1. Fluid inclusions in minerals from U deposits in Russia, Ukraine, and Kazakhstan.

(a–c) Druzhnoe deposit, Aldan, Russia (a, b—quartz, c—barite; homogenization temperatures T_h: a—245°C, b—210°C, c—238°C); (d–f) Strel'tsovskoe deposit, Transbaikalia, Russia (d—sphalerite, e—fluorite, f—barite, T_h = 184°C (d), 150°C (e), and 149°C (f)]; (g) Lastochka deposit, Far East, Russia (fluorite, T_h = 152°C, C = 4.7 wt % equiv. NaCl); (h) Zheltorechenskoe deposit, Ukraine (calcite, T_h = 168°C); (i–l) Molodezhnoe deposit, Kazakhstan (i–k)—calcite, T_h = 183°C (i), 179°C (j), 182°C (k), C = 6.9 wt % equiv. NaCl; (l)—quartz, T_h = 153°C, C = 9.1 wt % equiv. NaCl).

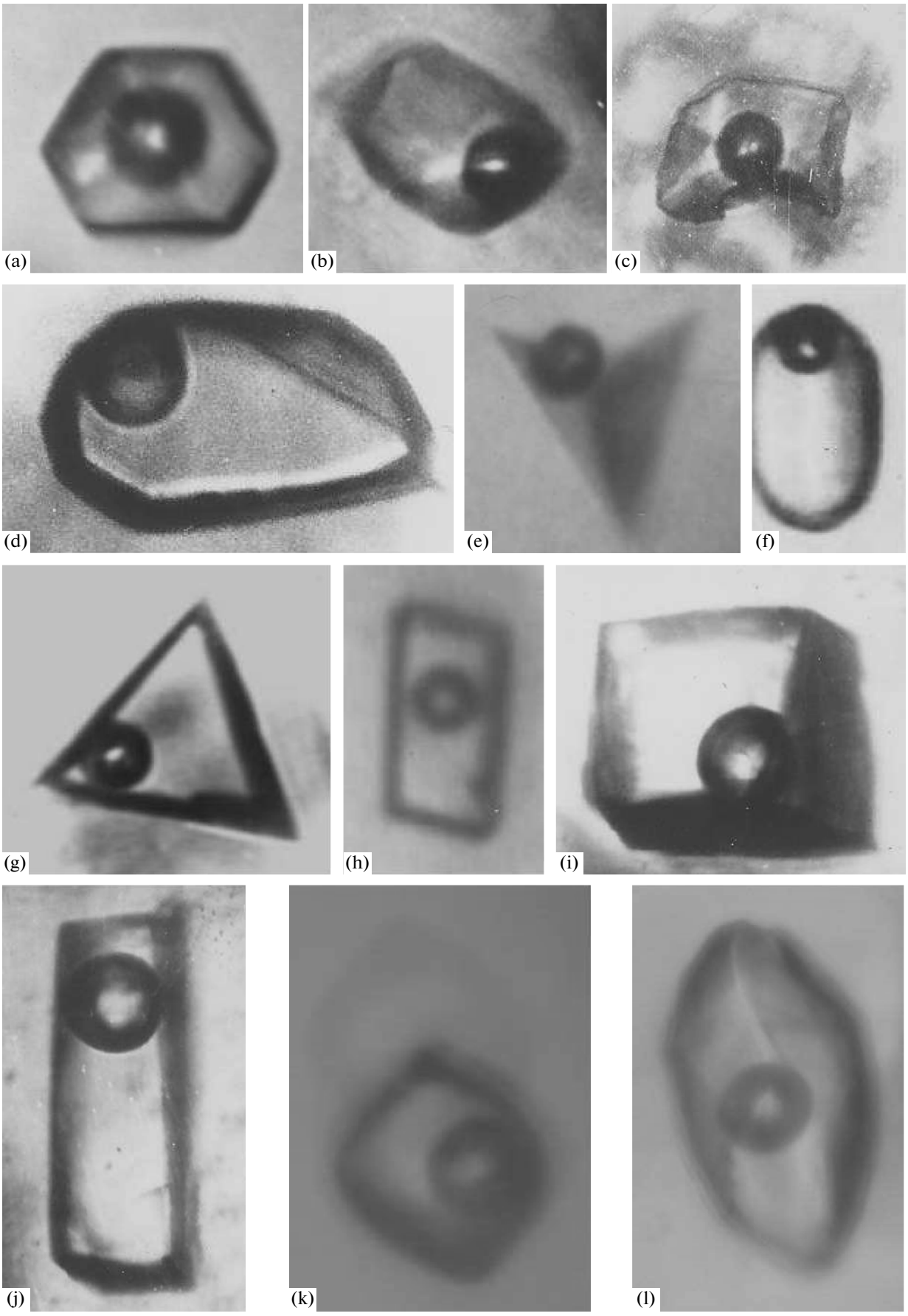
(a)
(b)
(c)
(d)
(e)
(f)
(g)
(h)
(i)
(j)
(k)
(l)

Table 2. Range of physicochemical parameters of fluids at U deposits determined by studying inclusions in minerals (literature data)

Deposit, region	Ore elements	Range of parameters			References
		T, °C	*P*, bar	C, wt %	
Tyuya-Muyun, Alai Range, S. Kirgizia	U, V	74–190	–	–	[6]
Strel'tsovskoe, Transbaikalia, Russia	U	125–175	–	–	[7]
Siberia, Russia	U	210–250	–	–	[8]
Tyuya-Muyun, Alai Range, S. Kirgizia	U, V	140–160	–	–	[9]
Orphan, Grand Canyon, Arizona, USA	U	45–124	–	–	[10]
Ukraine	U	120–490	–	–	[11]
Strel'tsovskoe, Transbaikalia, Russia	U	60–155	600–860	–	[12]
Echo Bay, Canada	U, Ni, Ag, Cu	120–160	–	–	[13]
Bois Noirs-Limoazat, Forez, France	U	98–100	–	16.0–20.0	[14]
Rabbit Lake, Atabaska, Canada	U	92–145	–	–	[15]
Ukraine	U	130–400	–	–	[16]
Rabbit Lake, Atabaska, Canada	U	130–160	700	28.0–30.0	[17]
Bois Noirs-Limoazat, Forez, France	U	40–350	–	1.0–25.0	[18]
Margnac and Fanay, France	U	45–107	–	1.9–2.0	[19]
Oklo, Gabon, Africa	U	111–440	–	2.6–25.5	[20]
Chateau-Lambert, S.Vosges, France	Cu, Mo, Ag, U	110–430	–	0.1–27.5	[21]
Ceara Precambrian, Brazil	U	108–117		19.8–25.0	[22]
Mistamisk Valley of the Labrador Trough, Quebec, Canada	U	325	2500	40.0	[23]
Schwartzwalder, Colorado, USA	U	75–165	–	3.0–19.0	[24]
North Canning, Owl Creek Mountains, Wyoming, USA	U	123–149	350	–	[25]
Ukraine	U	120–250	–	–	[26]
Oklo, Gabon, Africa	U	86–150	–	8.3–35.0	[27]
Northern Arizona, USA	U, Cu	80–173	–	10.1–17.5	[28]
Mary Kathleen, Queensland, Australia	U, REE	400–600	–	–	[29]
La Lauzier, Alps	U	180–245	–	8.0–19.6	[30]
Mohave County, Arizona, USA	U	104	–	9.9–16.4	[31]
Akouta, Nigeria, Africa	U	80–145	–	0.9–23.0	[32]
Slick Rock district., Colorado, USA	U, V	85–90	–	0.1–17.8	[33]
Cottonwood Wash, Utah, USA	U, V	90	–	–	[33]
Oklo, Gabon, Africa	U	113–155	–	2.6–6.4	[34]
Oklo, Gabon, Africa	U	112–132	–	25–33	[34]
Rabbit Lake, Saskatchewan, Canada	U	92–182	–	1.4–5.7	[34]
Cluff Lake, Saskatchewan, Canada	U	90–380	–	0.5–18.0	[34]
Cottonwood Wash, Utah, USA	U, V	100	–	2.1–8.5	[35]
Pribram, Bohemian Massif, Czechia	U	65–130	–	3.0	[36]
Rozna, Bohemian Massif, Czechia	U	100	–	2.0	[36]
Olympic Dam, Australia	Cu, U, Au, Ag	110–420	–	6.6–42.0	[37]
Akouta, Nigeria, Africa	U	85–175	–	8.0–23.0	[38]
Lodeve, France	U	95–110	–	22.4–28.0	[38]
Oklo, Gabon, Africa	U	112	–	19.5–40.0	[38]
Coronation Hill, Australia	Au, Pt, Pd, U	85–313	–	0.3–33.9	[39]
Capitan Mountains, New Mexico, USA	Th, U, REE	110–650	–	10.6–83.6	[40]
Athabasca Basin, Saskatchewan, Canada	U	30–280	–	–	[41]

Table 2. (Contd.)

Deposit, region	Ore elements	Range of parameters			References
		T, °C	*P*, bar	C, wt %	
El'kon district, Aldan Shield, Russia	U	200–230	–	–	[42]
Bernardan, France	U	54–360	–	–	[43]
Oklo, Gabon, Africa	U	160–468	–	0.2–17.8	[44]
Marysvale field, Utah, USA	U, Mo	113–272	–	0.1–2.1	[45]
Witwatersrand Basin, Southern Africa	Au, U	120–280	–	5.0–30.0	[46]
Kanimansur, Tajikistan	Ag, Pb, U, Cu, Zn, Bi	100–300	–	1.0–30.0	[47]
Malinovskoe, Kemerovskaya oblast, Russia	U	126–226	–	12.7–30.5	[48]
Lambapur-Peddagattu area, Andhra Pradesh, India	U	140–240	–	1.0–18.0	[49]
Sanerlin, Southern China	U	152–280	–	6.4–11.6	[50]
Witwatersrand conglomerates, Southern.Africa	Au, U	83–162	–	0.1–10.0	[51]
McArthur River, Saskatchewan, Canada	U	90–270	–	–	[52]
Kombolgie sandstones, Australia	U	87–240	875–1375	0.1–35.0	[53]
Karku, northern Ladoga area, Russia	U	87–261	–	0.4–42.7	[54]
McArthur River, Saskatchewan, Canada	U	170–235	400–1200	36.0–40.0	[55]
Southern McArthur basin, Northern Australia	U, Zn, Pb	83–230	–	0.1–30.9	[56]
Oak Dam East, Olympic Dam region, Southern Australia	Fe, Cu, Au, U	93–495	–	1.2–53.1	[57]
Alligator River Uranium Field, Australia	U	97–157	–	5.5–25.6	[58]
Oklo, Gabon, Africa	U	115–200	–	0.1–21.0	[59]
Zaohuohao area, Northern Ordos Basin, China	U	90–190	–	–	[60]
Southern China	U	150–250	–	1.3–8.9	[61]
Zalesi, Bohemian Massif, Czech Republic	U, Ni, Co, As, Ag, Bi	50–200	–	0.1–28.5	[62]
Rozna, Bohemian Massif, Czech Republic	U	107–206	–	0.5–25.3	[63]
Ordos Basin, NW China	U	79–193	–	0.4–16.3	[64]
Ordos Basin, NW China	U	58–176	–	–	[65]
Eva, Northern Australia	U	99–322	–	0.9–13.4	[66]
Jexson Pit, Northern Australia	U	99–322	–	0.9–14.4	[66]
Athabasca Basin, Canada	U	56–197	–	13.2–53.8	[67]
Novokonstantynivka, Central Ukraina	U	110–332	1600–2000	4.5–20.8	[68]
McArthur, Athabasca Basin, Saskatchewan, Canada	U	200–220	–	26.5–33.0	[69]
Bleilersgrund, Schwarzwald, SW Germany	Ag, Bi, Co, Ni, U	55–193	–	3.5–4.0	[70]
Emanuel, Schwarzwald, SW Germany	Ag, Bi, Co, Ni, U	58–132	–	15.0–19.5	[70]
Fluorspar, Schwarzwald, SW Germany	Ag, Bi, Co, Ni, U	60–150	–	10.0	[70]
Sophia, Schwarzwald, SW Germany	Ag, Bi, Co, Ni, U	60–390	–	1.7–24.5	[70]
Athabasca Basin, Canada	U	110–120	–	25–35	[71]
Rabbit Lake, Atabaska, Canada	U	122–222	–	27.3–29.7	[72]

C, wt % is the salinity of solution in wt % equiv. NaCl.

Table 3. Ranges of physicochemical parameter of fluids at U deposits determined by studying inclusion in minerals (our data)

Deposit, region	Mineral	Ranges of parameters		
		T, °C	*P*, bar	C, wt %
Zheltorechenskoe, Ukraine	Quartz (10)	230–350	1250–2300	–
"	Dolomite (3)	155–248	900–950	–
"	Calcite (3)	125–230	1250	–
Michurinskoe, Ukraine	Quartz (2)	240–250	1250–1360	–
"	Calcite (1)	142–147	–	–
Druzhnoe, Aldan, Russia	Quartz (5)	170–284	–	10.3
"	Barite (1)	230–265	–	–
"	Anhydrite (4)	185–230	340–700	–
"	Calcite (3)	100–255	–	–
"	Fluorite (2)	95–193	–	5.9
Vostok, Kazakhstan	Quartz (4)	98–166	–	–
"	Calcite (2)	124–155	–	–
Grachevskoe, Kazakhstan	Calcite (2)	228–243	–	–
Dergachevskoe, Kazakhstan	Calcite (1)	170–190	–	–
Ishim, Kazakhstan	Calcite (4)	72–171	–	–
"	Sphalerite (1)	110–130	–	–
Molodezhnoe, Kazakhstan	Axinite (1)	195–220	–	18.0
"	Quartz (5)	146–220	–	6.2–9.1
"	Calcite (4)	136–193	–	3.1–10.2
Strel'tsovskoe, Transbaikalia, Russia	Quartz (4)	142–226	320–670	–
	Ankerite (3)	179–205	–	–
"	Sphalerite (3)	172–214	–	7.5
"	Barite (2)	149–176	–	–
"	Fluorite (15)	120–179	–	–
"	Calcite (5)	58–177	–	–
"	Whewellite (1)	125–145	600–860	–
Dosatuiskoe, Transbaikalia	Fluorite (3)	150–191	–	–
Lastochka, Far East, Russia	Calcite (2)	187–197	–	–
Russia	Fluorite (3)	152–215	–	–
Schlema Alberoda, Germany	Quartz I (6)	280–320	480	–
"	Quartz II (3)	131–218	–	7.0
"	Sphalerite (3)	92–269	–	–
"	Ankerite (7)	114–156	–	25.1
"	Dolomite (3)	110–145	–	–
"	Siderite (10)	92–137	–	23.9
"	Calcite (17)	30–148	–	20.0–28.0
"	Fluorite (12)	95–230	–	–
"	Proustite (1)	40	–	–
"	Apophyllite (1)	40–80	–	–
"	Whewellite (1)	40	–	–
"	Barite (2)	40	–	–
Annaberg, Germany	Fluorite (3)	110–230	–	–

Table 3. (Contd.)

Deposit, region	Mineral	Ranges of parameters		
		T, °C	*P*, bar	C, wt %
Zobes, Germany	Calcite (1)	123–135	–	–
"	Fluorite (5)	95–195	–	–
Teleheuser, Germany	Fluorite (9)	86–204	–	–
Schneeberg, Germany	Sphalerite (1)	235–275	–	9.2–10.1
"	Quartz (1)	150–160	–	–
"	Calcite(1)	104–143	–	27.5
"	Anhydrite (1)	40	–	–
Pribram, Czech Republic	Fluorite (10)	125–160	–	–
"	Calcite (2)	35–60	–	
Katta sai, Uzbekistan	Quartz (2)	234–258	490	6.4
"	Sphalerite (4)	90–146	–	7.3–9.0
"	Fluorite (3)	120–250	–	–
Chauli, Uzbekistan	Fluorite (2)	210–268	–	4.2–14.0
"	Sphalerite (1)	102–112	–	14.0
"	Calcite (2)	112–171	–	0.3
"	Fluorite (1)	102–112	–	–
Dakhovskoe, Northern Caucasus,	Quartz (1)	168–170	–	–
Russia	Fluorite (2)	80–92	–	–
"	Ankerite (7)	60–96	–	–
"	Calcite (3)	44–70	–	–

Numerals in parentheses specify the number of studied samples; C, wt % is the salinity of solution in wt % equiv. NaCl.

torecehnskoe in Ukraine, Kata Sai in Uzbekistan, Druzhnoe in the Aldan Shield, and Strel'tsovskoe in Transbaikalia), quartz, anhydrite, and whewellite sometimes contain three-phase fluid inclusions consisting of aqueous solution, liquid carbon dioxide, and a gas phase. Their micrographs are presented in Fig. 3.

Figure 4 shows histograms of the homogenization temperatures of fluid inclusions in the most typical minerals at U deposits: quartz, fluorite, and calcite. Although the overall temperature range is broad, from low temperatures to 500°C, most of the measured values lie within a narrow range of 100–200°C. Table 4 summarizes data on the frequency of occurrence (in %) of temperature values within the range of 20–500°C and salinity values within the range of 0.1–50 wt % for hydrothermal mineral-forming fluids at U deposits. As can be seen in the table, 67% of the measured temperature values (937 individual measurements) fall within the range of 100–200°C.

Figure 5 summarizes representative enough data on the homogenization temperatures of fluid inclusions at U deposits (Fig. 5a, 1238 measured values), W deposits (Fig. 5b, 3538 measured values), and Sn deposits (Fig. 5c, 3292 measured values). As can be seen from these data, the temperatures at U deposits are remarkably lower. This feature, which distinguishes U deposits from deposits of other elements, is reflected in data of Table 5. The temperature range of 100–200°C includes

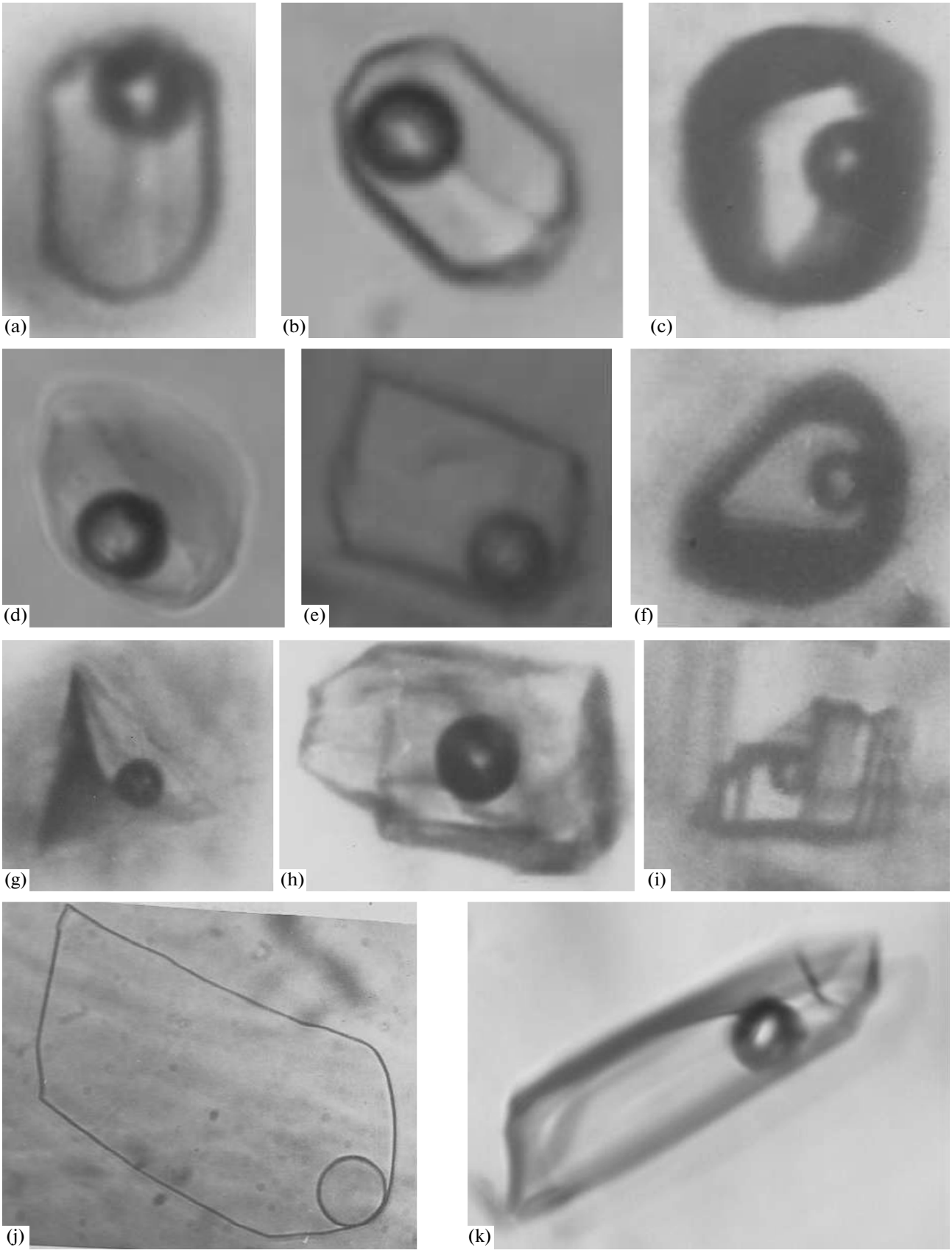
(a)
(b)
(c)
(d)
(e)
(f)
(g)
(h)
(i)
(j)
(k)

Fig. 2. Fluid inclusions in minerals from U deposits in Uzbekistan and Germany.

(a–c) Kata Sai deposit, Uzbekistan (a, b—quartz, c—sphalerite, T_h: a—245°C, b—245°C, C = 6.4 wt % equiv. NaCl, c—238°C); (d–f) Chauli deposit, Uzbekistan (d—fluorite, T_h = 210°C, C = 14.0 wt % equiv. NaCl; e—calcite, T_h = 158°C, C = 0.9 wt % equiv. NaCl; f—sphalerite, T_h = 110°C); (g–j) Schlema deposit, Germany (g—fluorite, T_h = 158°C; h—calcite, T_h = 122°C, i—siderite, T_h = 110°C; j—calcite, T_h = 109°C); K—Schneeberg deposit, calcite, T_h = 128°C, C = 27.5 wt % equiv. NaCl.

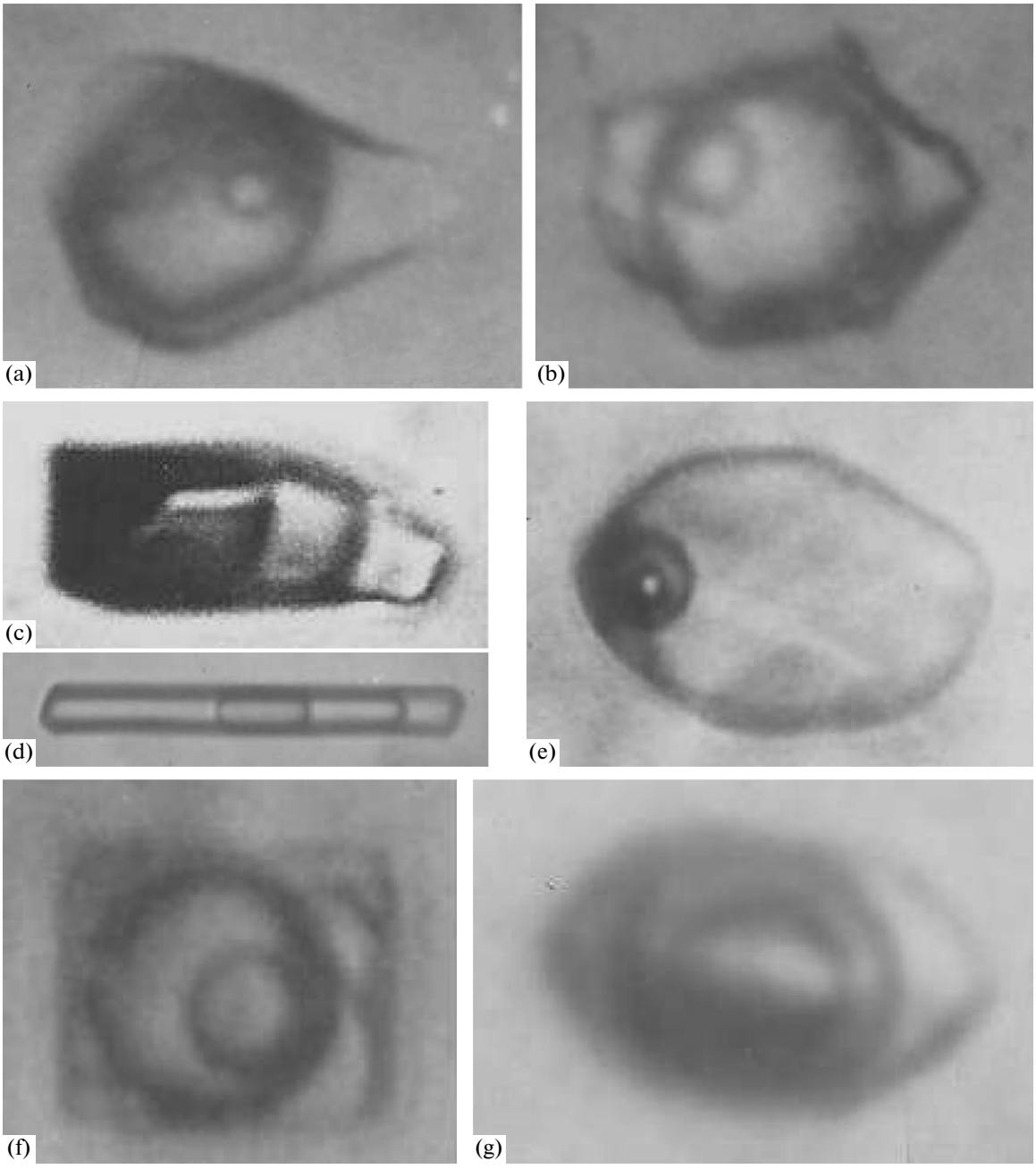

Fig. 3. Fluid inclusions with liquid CO_2 in minerals from U deposits in Ukraine, Russia, and Uzbekistan.

(a, b) Zheltorecehnskoe deposit, Ukraine (a—inclusion in quartz at +11°C, b—inclusion in quartz at –5°C); (c–e) Strel'tsovskoe deposit, Transbaikalia, Russia (c—quartz, temperature of partial homogenization into liquid is +31°C; d, e—whewellite, d—partial homogenization temperature is +11°C, e—T_h = 130°C); (f) Druzhnoe deposit, Aldan, Russia (inclusion in anhydrite); (g) Katta-Sai deposit, Uzbekistan (inclusion in quartz).

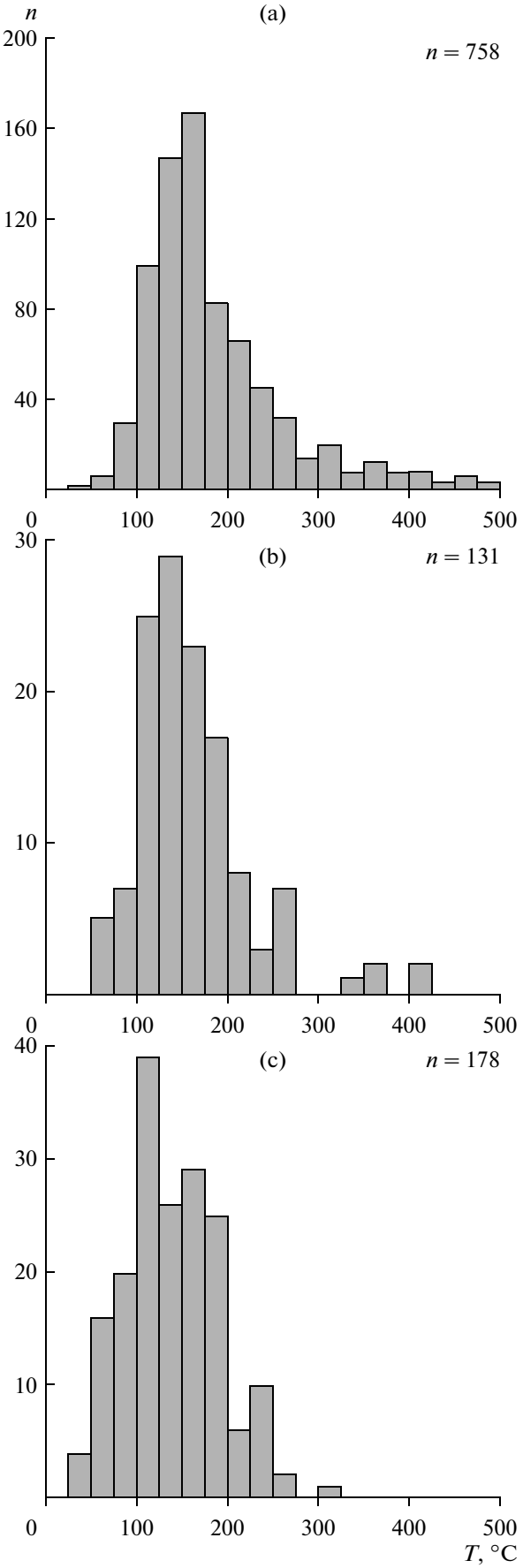

Fig. 4. Histograms of the homogenization temperatures of fluid inclusions in minerals from U deposits.
(a) Quartz, (b) fluorite, (c) calcite; *n*—number of measured values.

67% of all measured values for U deposits, 42% for base-metal deposits, 29% for Au–Ag deposits, and as little as 15% for W and Sn deposits.

PRESSURE OF MINERAL-FORMING FLUIDS

In contrast to fairly representative data on the temperature of fluids that produced U deposits, data on their pressure are relatively scarce. The 32 individual measured values are presented in Tables 2 and 3 and in Fig. 6. It is nevertheless obvious that fluid pressure was principally different at U deposits of different types. High pressure values of 900 to 2300 bar were determined at deposits in Ukraine (Zheltorechenskoe, Michurinskoe, and Novokonstantinovka). Equally high pressures (700–2500 bar) were detected at deposits in Canada [17, 23, 55] and Australia [53]. Intermediate pressure values of 300–800 bar were determined at other deposits ([25] and the Druzhnoe and Strel'tsovskoe deposits in Russia, Kata-Sai in Uzbekistan, and Schlema in Germany). We cannot rule out that fluid at some other deposits could have been under even lower pressures, but these cannot be determined in the absence of suitable techniques. It follows from Fig. 6 that the highest temperatures are correlated with the highest fluid pressures.

SALINITY AND DENSITY OF MINERAL-FORMING FLUIDS

Studying fluid inclusions in minerals offers a straightforward and reliable approach to determining the chemical composition, salinity, and density of mineral-forming fluids. Similar to data on fluid temperatures, much information is now accumulated on the salinity of naturally occurring fluids at U deposits throughout the world (Tables 2, 3). These data are summarized in Fig. 7, which shows a histogram of fluid salinity (Fig. 7a) and a correlation between fluid salinity and fluid temperature (Fig. 7b). Most of individual measured values are <10 wt % equiv. NaCl, and several values also lie within the range of 10–30 wt % equiv. NaCl. Table 4 reports the calculated frequency of occurrence of (in %) of temperature and salinity values of hydrothermal fluids at 20–500°C and 0.1–50 wt % equiv. NaCl. As was mentioned above, most measured values fall within the range of 0.1–0.5 wt % equiv. NaCl (28.7% of 937 measured values) and the next range of 5–10 wt % equiv. NaCl (20.7%). However, high salinity values (10–30 wt % equiv. NaCl) are typical of U deposits and account for 42% of all measurements. Table 5 shows differences between U deposits and deposits of other ore elements. The salinity range of 10–30 wt % equiv. NaCl

includes 42% of the measured values for U deposits (937 individual measurements), 27% for Au–Ag deposits (10 237 measurements), 27% for W deposits (2333 measurements), and 25% for Sn deposits (1981 measurements).

The relatively low temperatures of fluid at U deposits and the high salinity of this fluid testify that the solutions had a high density. Table 6 demonstrates the frequencies of occurrence (in %) calculated for the temperature and density values of hydrothermal fluids within the ranges of 20–500°C and 0.2–1.4 g/cm^3. These data indicate that 94% of all of the measured values lie within the range of 0.8–1.2 g/cm^3.

GAS COMPOSITION OF MINERAL-FORMING FLUIDS

Data on the composition of fluid inclusions at U deposits are not as abundant as data on fluids at deposits of other elements, largely because the former deposits contain relatively few minerals suitable for studying fluid inclusions in them. However, even information compiled from the scarce publications allowed us to derive important conclusions on the circumstances of U transportation and deposition. For example, complex carbonate compounds of hexavalent U are now thought to largely control U migration, the gas constituents of fluid inclusions were first of all analyzed for carbon dioxide [73, 74].

Analysis of variations in CO_2 concentrations during the processes that have produced pitchblende–carbonate veins at the Erzgebirge shows that systematic changes in the vein minerals (quartz–pitchblende–calcite) have been associated with a decrease in the CO_2 concentration from 100 g/kg of H_2O to 3–5 g/kg of H_2O. Pitchblende crystallization was associated with a continuous decrease in the carbon dioxide concentration of the solution, which reached a minimum after the ore deposition stage [73]. Carbon dioxide could be removed in two manners. The host rocks of the deep-sitting metasomatites could consume much carbon dioxide to form carbonates. At shallower depths, carbon dioxide was removed from the ore-forming solutions during their boiling when the pressure in the mineralized zone dropped.

The presence of CO_2 is not specific of U-bearing fluids. For example, four fluid types were distinguished in [46] in the Witwatersrand Basin, with the fluids evolving from early H_2O to H_2O–CO_2, then to H_2O–CH_4–CO_2, and eventually to CH_4–N_2. The latest multicomponent and multiphase fluids contained discernible concentrations of C_2H_6, C_3H_8, and H_2S. Table 7 reports Raman

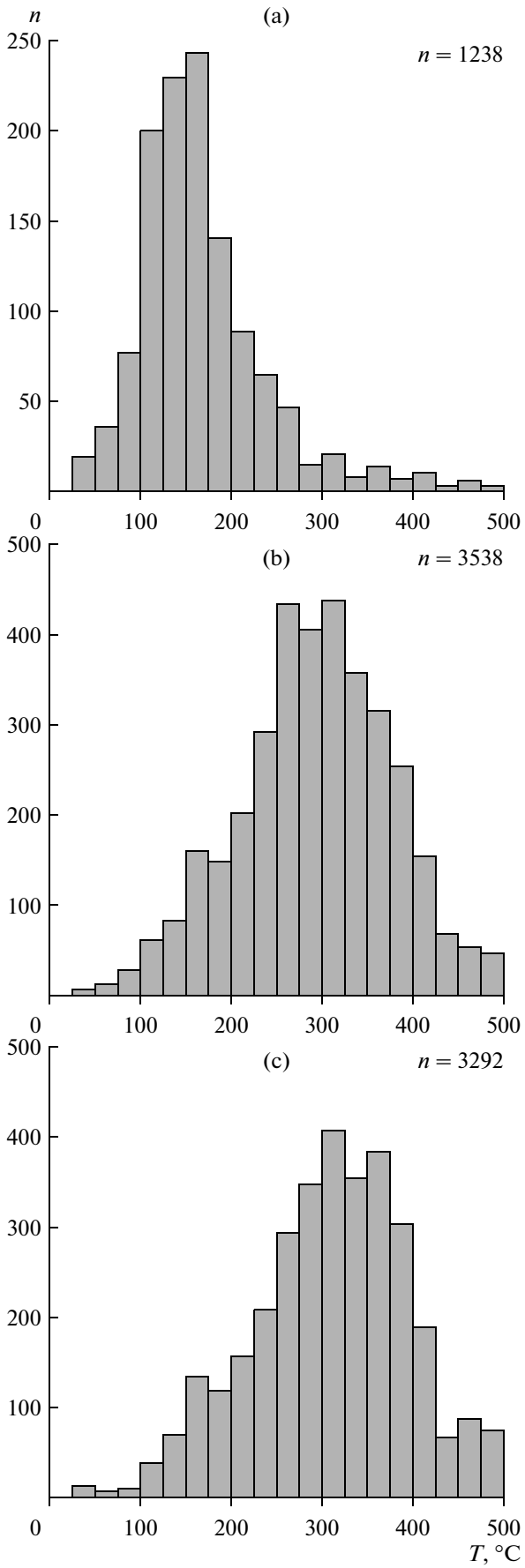

Fig. 5. Histograms of the homogenization temperatures of fluid inclusions in minerals from hydrothermal deposits. (a) U deposits, (b) W deposits, (c) Sn deposits; *n*—number of measured values.

Table 4. Frequency of occurrence (%) of temperature and salinity values of hydrothermal mineral-forming fluids within the ranges of 20–500°C and 0.1–50 wt % equiv. NaCl at U deposits (based on 937 individual analyses)

Salinity, wt %	Temperature, °C					
	20–100	100–200	200–300	300–400	400–500	20–500
0.1–5	2.7	20.6	4.6	0.8	–	28.7
5–10	1.4	13.0	5.0	1.1	0.3	20.7
10–15	0.9	8.7	1.3	0.7	0.2	11.8
15–20	1.4	6.2	1.3	0.3	0.1	9.3
20–25	1.4	9.2	0.8	0.1	–	11.5
25–30	0.7	6.3	2.2	–	0.1	9.2
30–35	0.2	2.4	2.5	0.3	0.1	5.5
35–40	0.2	0.7	0.2	–	–	1.2
40–45	–	0.3	0.2	0.4	0.1	1.1
45–50	–	0.1	0.2	0.1	0.6	1.0
0.1–50	8.9	67.5	18.3	3.8	1.5	100.0

spectroscopic analyses of the fluids, which are in reasonable agreement with microthermometric data. These results testify that fluid was trapped in minerals in several episodes, and the evolutionary history of the Witwatersrand Basin was complicated.

The very first studies of fluid inclusions have detected H_2S in the mineral-forming fluids, with this component detected first by cryometric techniques and then by direct analysis [75]. The wide application of Raman spectroscopy made such analyses usual, and information thus obtained testifies that hydrogen sulfide is widely involved in hydrothermal mineral-forming processes, including those generating U mineralization. When quartz from Witwatersrand [76] was studied, inclusions with high-density H_2S (0.79–0.81 g/cm^3) were found in this mineral. Quartz from mineralized veins in northern Kazakhstan was found out to contain inclusions of diverse types: pure H_2S (0.80 g/cm^3 in density), pure CO_2 (0.76–0.99 g/cm^3), and their mixes, which suggests that the fluids of the ore-forming hydrothermal systems may have originated from various sources [76].

When studying three Precambrian U deposits: Oklo in Gabon and Rabbit lake and Cluff Lake in Saskatchewan, Canada, Dubessy et al. [34] revealed an unusual composition of fluid inclusions by applying Raman spectroscopy (Table 8). Quartz samples from the natural nuclear reactor zone or its close vicinity at the Oklo deposit contained up to 100% H_2S, sometimes with traces of CH_4, in the anhydrous phase. Quartz near pitchblende from the Rabbit and Cluff deposits was proved to contain 79–99% O_2 in the gas phase, and the O_2/H_2 ratio of inclusions in it varied from 4 to 470, regardless of the volume proportions of the phases. These variations could occur when the inclusions were captured or result from variable hydrogen losses became of its high volatility. The actual reasons for these variations at these deposits, as several other uncertain issues, still await their elucidation.

The close spatial association of these unusual fluids with U ore mineralization suggest that it could result from water radiolysis. The process of water radiolysis in quartz from the Oklo deposit was later studied in much detail in [44]. It was demonstrated how much radiolysis in the presence of organic matter is able to modify local redox potential in natural nuclear reactor zones. The high effectiveness of radiochemical reactions suggests that radiolysis of water and/or organic matter may strongly affect processes generating fluids that can produce high U concentrations.

Samples of vein quartz and breccia collected in the vicinity of U ore and 50 m away from it at the McArthur River unconformity-type uranium deposit in Saskatchewan, Canada, were studied by Raman spectroscopy [52] to trace the redistribution of gas components with increasing distance from the orebody

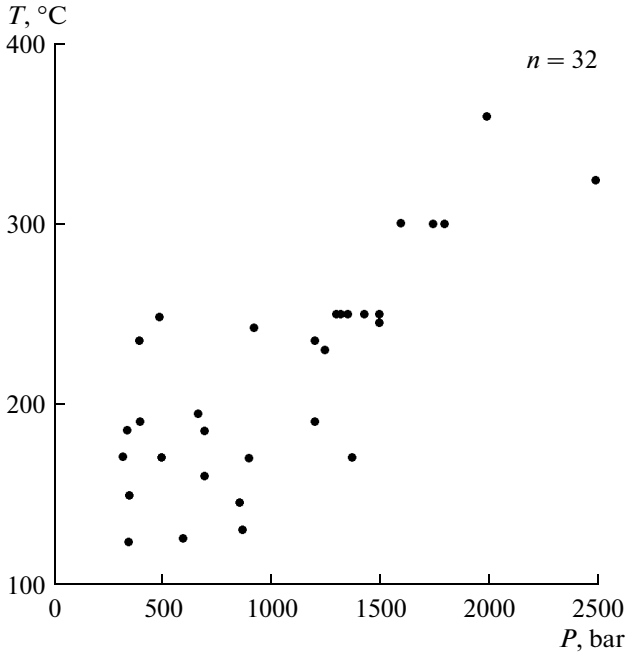

Fig. 6. Temperature and pressure values determined by studying fluid inclusions in minerals from U deposits.

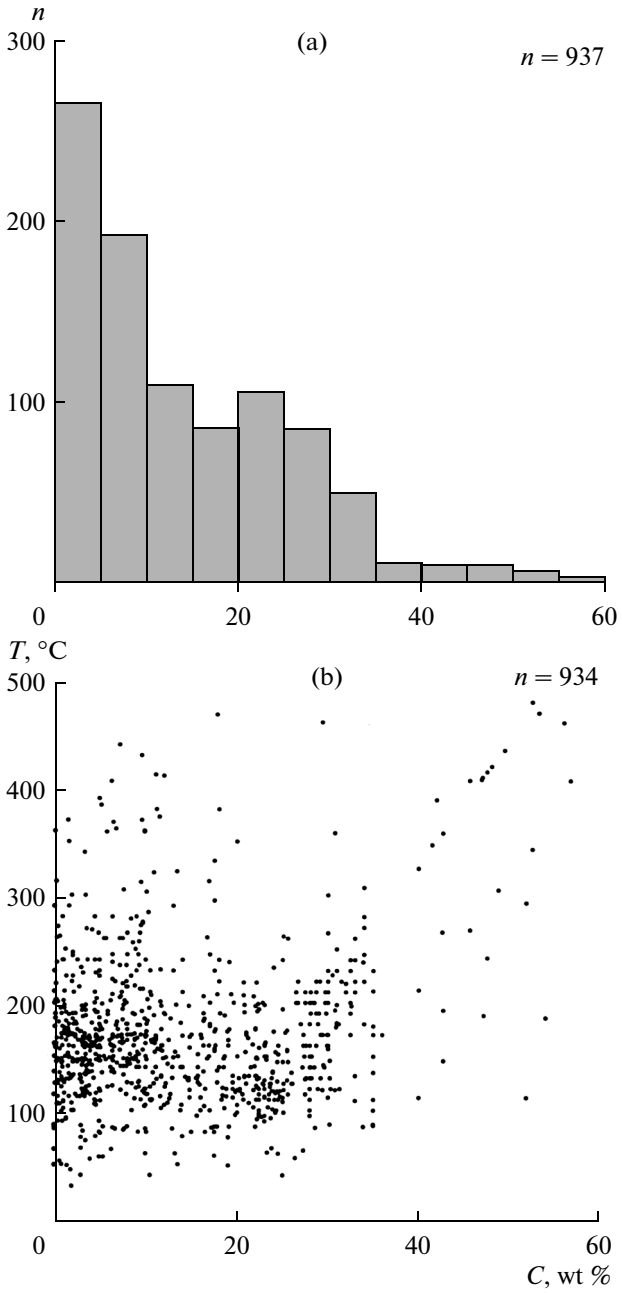

Fig. 7. Salinity of mineral-forming solutions at U deposits. (a) Histogram of the salinity of mineral-forming solutions; (b) temperature and salinity of mineral-forming solutions; *n* is the number of measured values.

(Table 9) and identify possible H_2 and O_2 sources in the gas phase of the fluid inclusions. The authors have analyzed four scenarios explaining the presence of H_2 and O_2 and concluded that the most probable scenario is heterogeneous entrapment of radiolysis products by fluid inclusions near U deposits. The further evolution of the gases was controlled by their different migration. The drastic decrease in the O_2 content in the inclusions away from the orebody may be explained by O_2 spending on the oxidation of the host rocks [44], as follows from the fact that hematite is often found near pitchblende accumulations.

The extremely high volatility of H_2 [34] makes it possible to reliably identify this gas in fluid inclusions at a distance from the U mineralization, and this can be used as a prospecting guide [52].

Extensive data on the composition of fluid inclusions in minerals at U deposits calls for their study in order to elucidate, after critical discussions, models for the genesis of and exploration for these deposits.

URANIUM CONCENTRATIONS IN NATURAL MAGMATIC MELTS AND FLUIDS

As was mentioned above, our database is composed of published data on fluid and melt inclusions. The database of concentrations of various elements in melt inclusions in minerals and in chilled glass of volcanic rocks now comprises more than 800 000 analyses for 74 elements [77]. The database on concentrations of elements in fluid inclusions in minerals consists of more than 48000 analyses for 72 elements. This provided us with the opportunity to estimate U concentrations in magmatic silicate melts and to compare these values with U concentration in fluids. To evaluate the average concentrations, we have preparatorily analyzed the type of their distribution. The latter was proved to be lognormal (Fig. 8), similar to the distributions of other elements, including volatiles and rare elements, we have determined earlier [77]. Because of this, the most probable values of the average U concentrations were

Table 5. Frequency of occurrence (%) of temperature and salinity values of hydrothermal mineral-forming fluids within the ranges of 20–500°C and 0.1–50 wt % equiv. NaCl at deposits of various elements

Range	U (937)	Pb, Zn (6459)	Au, Ag (10237)	W (2333)	Sn (1981)
Temperature					
20–100	8.9	9.6	2.5	1.2	0.4
100–200	67.5	41.8	29.3	15.1	14.6
200–300	18.3	33.4	42.4	36.9	33.9
300–400	3.8	13.1	21.5	37.6	38.7
400–500	1.5	2.1	4.3	9.2	12.4
Salinity					
0.1–10	49.4	48.1	64.5	62.8	62.0
10–20	21.1	25.0	18.5	21.3	16.5
20–30	20.7	21.8	8.4	6.2	8.8
30–40	6.7	4.2	5.9	6.3	9.7
40–50	2.1	0.9	2.7	3.4	3.0

Numerals in parentheses specify the numbers of measured values.

Table 6. Frequency of occurrence (%) of temperature and density values of hydrothermal mineral-forming fluids within the ranges of 20–500°C and 0.2–1.4 g/cm^3 at U deposits (based on 937 individual analyses)

Density, g/cm^3	Temperature, °C					
	20–100	100–200	200–300	300–400	400–500	20–500
0.2–0.4	–	–	–	–	0.1	0.1
0.4–0.6	–	–	–	0.4	0.2	0.6
0.6–0.8	–	–	0.8	1.6	0.3	2.7
0.8–1.0	1.3	34.1	11.0	1.0	0.3	47.7
1.0–1.2	6.9	31.3	6.2	0.6	1.1	46.1
1.2–1.4	0.5	1.5	0.2	0.5	0.1	2.8
0.2–1.4	8.7	66.9	18.2	4.1	2.1	100.0

assumed as the arithmetic mean values of their logarithms, i.e., geometric mean values. We have also calculated the confidence ranges corresponding to 0.95 confidence probability, and these values are represented in a natural form for convenience (the numeral before the virgule corresponds to the average plus and the numeral after it shows the average minus).

The geometric average U concentration of silicate melts (based on the data of 8053 individual analyses) is 0.92 ppm (+6.37/–0.80), and the average U concentration of hydrothermal fluids (271 individual analyses) is 1.21 ppm (+20.24/–1.14). Uranium concentrations in melts significantly vary with their silicity (Table 10). The average U concentration in mafic melts (SiO_2 = 40–54 wt %) is 0.29 ppm, whereas silicic melts contain 16 times more U: 4.64 ppm.

In addition to mean U concentrations in melts and fluids, it is interesting to discuss the maximum U con-

Table 7. Raman spectroscopic analyses of fluid inclusions in quartz from Witwatersrand, South Africa [46]

Sample	H_2O	CO_2	CH_4	N_2	H_2S
1	97.50	0.77	0.27	0.00	0.00
2	92.86	5.24	0.00	0.00	0.00
3	91.74	4.13	0.00	0.00	0.00
4	83.69	14.79	0.00	0.00	0.00
5	0.00	9.36	79.36	10.66	0.60
6	38.94	6.16	48.11	6.45	0.36

Table 8. Composition of the gas phase of fluid inclusions in quartz form U deposits [34]

n	H_2	O_2	CO_2	CH_4	N_2
Oklo					
5	>99.6	0	0	<0.4	0
2	100	0	0	0	0
1	100	0	0	0	0
1	31	0	69	0	0
2	100	0	0	0	0
Rabbit lake					
11	4.5	94.5	0	0	0
Cluff Lake					
3	10	90	0	0	0

n is the number of measured values.

Table 9. Variations in the composition of the gas phase of fluid inclusions with increasing distance from the orebody [52]

Distance	*n*	CO_2	CH_4	C_2H_6	H_2	O_2
<1 cm	8	n.d.	n.d.	n.d.	10.8	89.2
approximately 1 m	25	n.d.	0.5	n.d.	70.2	29.3
approximately 10 m	20	5.8	39.4	1.0	52.0	1.8
50 m	2	n.d.	n.d.	n.d.	100.0	n.d.

n is the number of measured values, n.d. denotes concentrations below the detection limits.

Table 10. U concentrations (ppm) in silicate melts and hydrothermal fluids determined by studying inclusions in minerals and chilled glasses of rocks

Silicate melts				Hydrothermal fluids
Mafic SiO_2 = 40–54 wt %	Intermediate SiO_2 = 54–66 wt %	Acid SiO_2 > 66 wt %	All SiO_2 > 40 wt %	
0.29	0.86	4.64	0.92	1.21
+0.70/–0.20	+ 2.18/–0.62	+6.76/–2.75	+6.37/–0.80	+20.24/–1.14
n = 4726	*n* = 567	*n* = 2760	*n* = 8053	*n* = 271

n is the number of measured values. U concentration was calculated as a geometric mean if individual measured values did not deviate from the mean value for more than 2σ at 95% probability. Numerals below mean values denote deviations (mean plus/mean minus).

Table 11. Ranges of U concentrations (ppm) in natural silicate melts and hydrothermal fluids (with references to publications reporting the maximum U concentrations)

Concentration in melt	*n*	Reference	Concentration in fluid	*n*	Reference
315–3.3	15	[77]	450–0.2	40	[84]
219–6.3	5	[78]	190	1	[85]
162–13.0	3	[79]	51–1.0	21	[86]
155	1	[80]	44–1.4	3	[87]
131–2.0	32	[81]	42–1.9	12	[88]
95–5.9	84	[82]	32–0.1	43	[89]
117–4.4	26	[83]	19–1.0	7	[90]

n is the number of measured values.

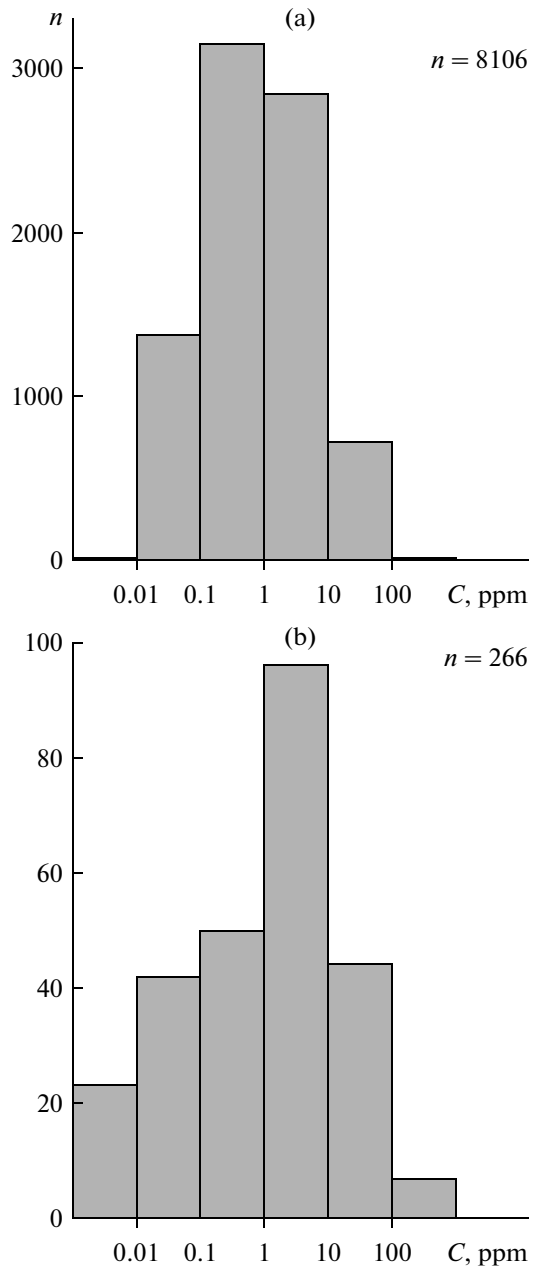

Fig. 8. Histograms of U concentration in (a) silicate magmatic melts and (b) natural fluids; *n* is the number of measured values.

centrations, which were reported in certain publications. Table 11 presents such data, which indicate that U concentrations reach a maximum of 200–300 ppm in silicate melts and 200–450 ppm in hydrothermal fluids.

We believe that data (based on representative results of studying fluid inclusions) on the principal physicochemical parameters of mineral-forming fluids should be taken into account when genetic models are suggested for the genesis of U deposits.

CONCLUSIONS

1. The paper presents a review and discussion of the principal physicochemical parameters (temperature, pressure, density, salinity, gas composition, and U concentrations in fluids) under which 90 hydrothermal U deposits and occurrences were formed. Temperatures most favorable for the generation of these deposits lie within the range of 100–200°C, which makes U deposits remarkably different from higher temperature base-metal, Au–Ag, W, and Sn deposits.

2. Solutions at U deposits are proved to have a high salinity: 42% of all measured values (937 analyses) fall within the range of 10–30 wt % equiv. NaCl, which also distinguishes U deposits from Au–Ag ones (25% of 10237 analyses), W deposits (27% of 2333 analyses), and Sn deposits (25% of 1981 analyses). The relatively low temperatures of U-bearing fluids and their high salinity testify that the solutions had a high density: 94% of all measured values fall within the range of 0.8–1.2 g/cm^3. The fluid pressure broadly varied from 2500 to 300 bar and, perhaps, even to lower values.

3. Data on the chemical composition of the gas phase of the fluid inclusions reveal the compositional diversity of these inclusions. In certain instances, H_2O–CO_2 fluids gave way to fluids rich in CH_4 and N_2 and containing trace amounts of hydrocarbons. We have also revealed distinguishing features of the gas composition of fluid inclusions from the nuclear-reactor zones of three Precambrian U deposits.

4. Individual analyses of inclusions were utilized to evaluate U concentrations in magmatic melts and mineral-forming fluids. The geometric mean U concentration for silicate melts of any composition is 0.92 ppm (based on 8053 individual analyses), and the analogous value for fluids is 1.21 ppm (271 analyses).

ACKNOWLEDGMENTS

The authors thank V.Yu. Prokof'ev for help with cryometric studies of fluid inclusions. This study was financially supported by the Russian Foundation for Basic Research, project no. 13-05-00450.

REFERENCES

1. V. B. Naumov, V. A. Dorofeeva, and O. F. Mironova, "Principal physicochemical parameters of natural mineral-forming fluids," Geochem. Int., **47** (8), 777–802 (2009).
2. O. F. Mironova, "Volatile components of natural fluids: evidence from inclusions in minerals: methods and results," Geochem. Int. **48** (1), 83–90 (2010).
3. V. B. Naumov, V. A. Dorofeeva, and O. F. Mironova, "Physicochemical parameters of the formation of hydrothermal deposits: a fluid inclusion study. I. Tin and tungsten deposits," Geochem. Int., **49** (10), 1002–1021 (2011).
4. V. B. Naumov, V. A. Dorofeeva, and O. F. Mironova, "Physicochemical formation parameters of hydrother-

mal mineral deposits: evidence from fluid inclusions. II. Gold, silver, lead, and zink deposits," Geochem. Int. **52** (6), 433–455 (2014).

5. A. I. Tugarinov and V. B. Naumov, "*P–T* conditions of formation of hydrothermal uranium deposits," Geokhimiya, No. 2, 131–146 (1969).
6. N. P. Ermakov, "*Study of Mineral-Forming Solutions*, (Khar'kovsk. Univ., Khar'kov, 1950) [in Russian].
7. V. F. Lesnyak and A. A. Lokerman, "Some results of mineralogical thermometric study of fluorite deposits in eastern Transbaikalia," Mineral. Sb. L'vovsk. Gos. Uninv., No. 19, 476–481 (1965).
8. N. A. Kulik, "Joint simultaneous growth of uraninite and brannerite and some data on conditions of formation of uranium minerals," in *Geochemistry and Mineralogy of Radioactive Elements of Siberia* (Nauka, Novosibirsk, 1970), pp. 17–53 [in Russian].
9. N. N. Smolyaninova, "Some data on the mineralogy and genesis of the Tyuya-Muyun deposit," in *Essays on Geology and Geochemistry of Ore Deposits* (Nauka, Moscow, 1970), pp. 58–90 [in Russian].
10. V. Gornitz and P. F. Kerr, "Uranium mineralization and alteration of Orphan Mine, Grand Canyon, Arizona," Econ. Geol. **65**, 751–768 (1970).
11. G. B. Naumov, A. A. Nikitin, and V. B. Naumov, "Hydrothermal whewellite from fluorite veins in Transbaikalia and conditions of its genesis," Geokhimiya, No. 2, 180–186 (1971).
12. N. P. Grishichnikov, V. A. Zinchenko, O. A. Kramar, O. F. Makivchuk, N. V. Smolin, N. I. Popov, F. D. Galkin, A. S. Ionov, V. I. Volkov, and Yu. P. Shestakov, "Structural features and evolution of a mineral deposit of the sodium–uranium formation," Geol. Zh., No. 4, 56–64 (1973).
13. B. W. Robinson and H. Ohmoto, "Mineralogy, fluid inclusions, and stable isotopes of the Echo Bay U–Ni–Ag–Cu deposits, Northwest Territories, Canada," Econ. Geol. **68**, 635–656 (1973).
14. B. P. Poty, M. Cuney, and J. Leroy, "Gas–Liquid inclusions in minerals from the Limousine and Forez uranium deposits confined to the Central French Granitoid Massif," in *Genesis of Uranium Deposits* (Mir, Moscow, 1976), pp. 583–596 [in Russian].
15. M. Pagel, "Conditions de depot des quartz et dolomites automorphes du gisement uranifere de Rabbit Lake (Canada)," *4-Eme Reun Annu. Sci. Terre* (Paris, 1976).
16. N. P. Grechishnikov, O. A. Kramar, S. V. Kuznetsova, O. F. Makivchuk, V. I. Nikolaenko, V. N. Obrizanov, and N. I. Popov, "Features of hypogenic zonning in one of the deposits of sodium–uranium formations," Geol. Zh., No. 3, 61–69 (1977).
17. M. Pagel and H. Jaffrezic, "Analyses chimiques des saumures des inclusions du quartz et de la dolomite du gisement d'Uranium de Rabbit Lake (Canada). Aspect methodologique et importance genetique," C.R. Acad.Sci., Ser. D **284** (2), 113–116 (1977).
18. M. Cuney, "Geologie environment, mineralogy, and fluid inclusions of the Bois Noirs-Limouzat uranium vein, Forez, France," Econ. Geol. **73**, 1567–1610 (1978).
19. J. Leroy, "The Margnac and Fanay uranium deposits of the La Crouzille district (Western Massif Central, France): geologic and fluid inclusion studies," Econ. Geol. **73**, 1611–1634 (1978).
20. R. Openshaw, M. Pagel, and B. Poty, "Phases fluides contemporaines de la diagenese des gres, des mouvements tectoniques et du fonctionnement des reacteurs nucleaires d'Oklo (Gabon)," *React. Fission Natur. C.R.Reun Com. Techn.* (Vienna, 1978), pp. 267–296.
21. M. Pagel and F. Ruhlmann, "Mineralogie et inclusions fluides dans les formations filoniennes mineralisees (Cu, Mo, Ag, U) du secteur de Chateau-Lambert (Vosges Meridionales)," Bull. Mineral. **102**, 654–664 (1979).
22. A. G. Angeiras, A. M. Netto, and M. De Campos, *Phospho-uraniferous mineralization associated with sodium episyenites in the Ceara Precambrian (Brazil), in Uranium Deposits in Latin America: Geology and Exploration* (Vienna, 1981), pp. 555–580.
23. L. Kish and M. Cuney, "Uraninite–albite veins from the Mistamisk Valley of the Labrador Trough, Quebec," Mineral. Mag. **44**, 471–483 (1981).
24. R. Rich and A. H. Barabas, "Genetic implication of preliminary mineralogical, paragenetic and fluid inclusion data for the Schwartzwalder Uranium Mine, Colorado," in *Vein-Type and Similar Uranium Deposits Rocks Younger than Proterozoic. Proc. Techn. Comm. Meet., Lisbon, Protugal, 1979* (Vienna, 1982), pp. 181–192.
25. T. Shrier and W. T. Parry, "A hydrothermal model for the North Canning uranium deposit, Owl Creek Mountains, Wyoming," Econ. Geol. **77**, 632–645 (1982).
26. I. P. Shcherban and V. V. Shun'ko, "Chlorite–orthoclase wall-rock metasomatites at the uranium occurrences," Geol. Rudn. Mestorozhd., No. 3, 43–54 (1983).
27. F. Gauthier-Lafaye and F. Weber, "Effets des deformations posterieures a une diagenese siliceuse d'enfouissement sur le comportement microthermometrique des inclusons fluides: cas du reservoir Greseux Uranifere du Francevillien(Gabon)," C.R. Acad. Sci., Ser. 2 **299**, 555–560 (1984).
28. K. J. Wenrich, "Mineralization of breccia pipes in northern Arizona," Econ. Geol. **80**, 1722–1725 (1985).
29. T. A. P. Kwak, W. M. Brown, P. B. Abeysinghe, and T. H. Tan, "Fe solubilities in very saline hydrothermal fluids: their relation to zoning in some ore deposits," Econ. Geol. **81**, 447–465 (1986).
30. H. S. Negga, S. M. F. Sheppard, J. M. Rosenbaum, and M. Cuney, "Late Hercynian U-vein mineralization in the Alps: fluid inclusion and C, O, H isotopic evidence for mixing between two externally derived fluids," Contrib. Mineral. Petrol. **93**, 179–186 (1986).
31. J. D. Rasmussen, C. G. Cunningham, and A. M. Gautier, "Primary fluid inclusions in sphalerite from the Hack 1 and 2 mines, Mohave County, Arizona," Geol. Soc. Am. Abstr. with Programs **18**, 404 (1986).
32. P. Forbes, P. Landais, M. Pagel, and A. Meyer, "Thermal evolution of the Guezouman Formation in the Akouta uranium deposit (Niger)," Terra Cognita **7**, 343 (1987).
33. J. D. Meunier and G. N. Breit, "Fluid inclusion studies in calcite associated with sandstone-hosted uranium–vanadium deposits of the Colorado Plateau," Fluid Incl. Res. **20**, 266 (1987).

34. J. Dubessy, M. Pagel, J.-M. Beny, H. Christensen, B. Hickel, C. Kosztolanyi, B. Poty, "Radiolysis evidenced by H_2–O_2 and H_2-bearing fluid inclusions in three uranium deposits," Geochim. Cosmochim. Acta **52**, 1155–1167 (1988).
35. B. Poty and M. Pagel, "Fluid inclusions related to uranium deposits: a review," J. Geol. Soc. **145**, 157–162 (1988).
36. K. Zak, P. Dobes, and P. Sztacho, "Variscan and Late Variscan vein mineralization types of the Czech Part of the Bohemian Massif: a genetic model," in *Source, Transport and Deposition of Metals*, Ed. by M. Pagel and J. Leroy (Balkema, Rotterdam, 1991).
37. N. Oreskes and M. T. Einaudi, "Origin of hydrothermal fluids at Olympic Dam: preliminary results from fluid inclusions and stable isotopes," Econ. Geol. **87**, 64–90 (1992).
38. M. Pagel, "Transport of uranium by sedimentary brines at temperatures between 80°C and 200°C," in *Current Research in Geology Applied to Ore Deposits. Proceedings SGA Meeting, Spain, 1993* (Spain, Granada, 1993).
39. T. P. Marnagh, C. A. Heinrich, J. P. Leckie, D. P. Carville, D. J. Gilbert, R. K. Valenta, and L. A. I. Wyborn, "Chemistry of low-temperature hydrothermal gold, platinum, and palladium (uranium) mineralization at Coronation Hill, Northern Territory, Australia," Econ. Geol. **89**, 1053–1073 (1994).
40. A. R. Campbell, D. A. Banks, R. S. Phillips, and B. W. D. Yardley, "Geochemistry of Th–U–REE mineralizing magmatic fluids, Capitan Mountains, New Mexico," Econ. Geol. **90**, 1271–1287 (1995).
41. T. G. Kotzer and T. G. Kyser, "Petrogenesis of the Proterozoic Athabasca Basin, Northern Saskatchewan, Canada, and its relation to diagenesis, hydrothermal uranium mineralization and paleohydrogeology," Chem. Geol. **120**, 45–89 (1995).
42. A. K. Miguta, "Composition and mineral assemblages of uranium ores in the El'kon District, Aldan Shield (Russia)," Geol. Ore Dep. **38**, 275–293 (1997).
43. P. Patrier, D. Beaufort, H. Bril, M. Bonhomme, A. M. Fouillac, and R. Aumaitre, "Alteration–mineralization at the Bernardan U Deposit (Western Marche, France): the contribution of alteration petrology and crystal chemistry of secondary phases to a new genetic model," Econ. Geol **92**, 448–467 (1997).
44. V. Savary and M. Pagel, "The effects of water radiolysis on local redox conditions in the Oklo, Gabon, natural fission reactors 10 and 16," Geochim. Cosmochim. Acta **61**, 4479–4494 (1997).
45. C. G. Gunningham, J. D. Rasmussen, T. A. Steven, R. O. Rye, P. D. Rowley, S. B. Romberger, and J. Selverstone, "Hydrothermal uranium deposits containing molybdenum and fluorite in the Marysvale volcanic field, West-Central Utah," Miner. Deposita **33**, 477–494 (1998).
46. G. R. Drennan, M. -C. Boiron, M. Cathelineau, and L. J. Robb, "Characteristics of post-depositional fluids in the Witwatersrand Basin," Mineral. Petrol. **66**, 83–109 (1999).
47. Yu. G. Safonov, N. S. Bortnikov, T. M. Zlobina, V. F. Chernyshev, A. B. Dzainukov, and V. Yu. Prokof'ev, "Polymetal (Ag, Pb, U, Cu, Bi, Zn, F) Adrasman–Kanimansur ore field (Tadzhikistan), and its ore-forming system. I: Geology, mineralogy, and structural conditions of the ore deposition," Geol. Ore Dep. **42**, 350–362 (2000).
48. S. F. Vinokurov, O. A. Doinikova, T. L. Krylova, V. V. Men'shikov, M. V. Nesterova, B. I. Ryzhov, and A. N. Sysoev, "Lithological–geochemical features of the Malinovskoe Uranium Deposit (Russia)," Geol. Ore Dep. **43**, 371–385 (2001).
49. B. S. Bisht, P. Rajasekaran, and R. M. Sinha, "Fluid inclusion characteristics of unconformity-related uranium mineralisation, Lambapur–Peddagattu Area, Andhra Pradesh," J. Geol. Soc. India **58**, 45–51 (2001).
50. J.-W. Li, M. -F. Zhou, X. -F. Li, Z.-J. Li, and Z. R. Fu, "Origin of a large breccia-vein system in the Sanerlin uranium deposit, southern China: a reinterpretation," Miner. Deposita **37**, 213–225 (2002).
51. A. Vollbrecht, T. Oberthur, J. Ruedrich, and K. Weber, "Microfabric analyses applied to the Witwatersrand gold- and uranium-bearing conglomerates: constraints on the provenance and post-depositional modification of rock and ore components," Miner. Deposita **37**, 433–451 (2002).
52. D. Derome, M. Cathelineau, T. Lhomme, and M. Cuney, "Fluid inclusion evidence of the differential migration of H_2 and O_2 in the McArthur River unconformity-type uranium deposit (Saskatchewan, Canada). Possible role on post-ore modifications of the host rocks," J. Geochem. Explor. **78–79**, 525–530 (2003).
53. D. Derome, M. Cuney, M. Cathelineau, C. Fabre, J. Dubessy, P. Bruneton, and A. Hubert, "A detailed fluid inclusion study in silicified breccias from the Kombolgie sandstones (Northern Territory, Australia): inferences for the genesis of Middle-Proterozoic unconformity-type uranium deposits," J. Geochem. Explor. **80**, 259–275 (2003).
54. V. I. Velichkin, V. K. Kushnerenko, N. N. Tarasov, O. V. Andreeva, G. D. Kiseleva, T. L. Krylova, O. A. Doinikova, V. N. Golubev, and V. A. Golovin, "Geology and formation conditions of the Karku unconformity-type deposit in the northern Ladoga Region (Russia)," Geol. Ore Dep. **47**, 87–112 (2005).
55. D. Derome, M. Cathelineau, M. Cuney, C. Fabre, T. Lhomme, and D. A. Banks, "Mixing of sodic and calcic brines and uranium deposition at McArthur River, Saskatchewan, Canada: a Raman and laser-induced breakdown spectroscopic study of fluid inclusions," Econ. Geol. **100**, 1529–1545 (2005).
56. P. A. Polito, T. K. Kyser, and M. J. Jackson, "The role of sandstone diagenesis and aquifer evolution in the formation of uranium and zinc–lead deposits, Southern McArthur Basin, Northern Territory, Australia," Econ. Geol. **101**, 1189–1200 (2006).
57. G. J. Davidson, H. Paterson, S. Meffre, and R. F. Berry, "Characteristics and origin of the Oak Dam East Breccia-Hosted, iron oxide Cu–U–(Au) deposit: Olympic Dam Region, Gawler Craton, South Australia," Econ. Geol. **102**, 1471–1498 (2007).
58. D. Derome, M. Cathelineau, C. Fabre, M.-Ch. Boiron, D. Banks, T. Lhomme, and M. Cuney, "Paleo-fluid composition determined from individual fluid inclusions by Raman and LIBS: application to Mid-Proterozoic evaporitic Na–Ca brines (Alligator Rivers uranium field, Northern Territories Australia)," Chem. Geol. **237**, 240–254 (2007).

59. A. Dutkiewicz, S. C. George, D. J. Mossman, J. Ridley, and H. Volk, "Oil and its biomarkers associated with the Palaeoproterozoic Oklo natural fission reactors, Gabon," Chem. Geol. **244**, 130–154 (2007).
60. H. J. Gan, X. M. Xiao, Y. C. Lu, Y. B. Jin, H. Tian, and D. H. Liu, "Genetic relationship between natural gas dispersal zone and uranium accumulation in the Northern Ordos Basin, China," Acta Geol. Sinica **81** (3), 501–509 (2007).
61. R. Z. Hu, X. W. Bi, M. F. Zhoi, J. T. Peng, W. C. Su, S. Liu, and H. W. Qi, "Uranium metallogenesis in south China and its relationship to crustal extension during the Cretaceous to Tertiary," Econ. Geol. **103**, 583–598 (2008).
62. Z. Dolnicek, B. Fojt, W. Prochaska, J. Kucera, and P. Sulovsky, "Origin of the Zalesi U–Ni–Co–As–Ag/Bi deposit, Bohemian Massif, Czech Republic: fluid inclusion and stable isotope constraints," Miner. Deposita **44**, 81–97 (2009).
63. B. Kribek, K. Zak, P. Dobes, J. Leichmann, M. Pudilova, M. Rene, B. Scharm, M. Scharmova, A. Hajek, D. Holeczy, U. F. Hein, and B. Lehmann, "The Rozna uranium deposit (Bohemian Massif, Czech Republic): shear zone-hosted, Late Variscan and Post-Variscan hydrothermal mineralization," Miner. Deposita **44**, 99–128 (2009).
64. X. Y. Yang, M. X. Ling, W. D. Sun, X. D. Luo, X. D. Lai, C. Y. Liu, J. Y. Miao, and W. Sun, "The genesis of sandstone-type uranium deposits in the Ordos Basin, NW China: constraints provided by fluid inclusions and stable isotopes," Int. Geol. Rev. **51**, 422–455 (2009).
65. C. J. Xue, G. X. Chi, and W. Xue, "Interaction of two fluid systems in the formation of sandstone-hosted uranium deposits in the Ordos Basin: geochemical evidence and hydrodynamic modeling," J. Geochem. Explor. **106**, 226–235 (2010).
66. T. P. Mernagh and E. S. Wygralak, "A fluid inclusion study of uranium and copper mineral systems in the Murphy Inlier (northern Australia)," Russ. Geol. Geophys. **52** (11), 1421–1435 (2011).
67. A. Richard, D. A. Banks, J. Mercadier, M.-Ch. Boiron, M. Cuney, and M. Cathelineau, "An evaporated seawater origin for the ore-forming brines in unconformity-related uranium deposits (Athabasca Basin, Canada): Cl/Br and ^{37}Cl analysis of fluid inclusions," Geochim. Cosmochim. Acta **75**, 2792–2810 (2011).
68. M. Cuney, A. Emetz, J. Mercadier, V. Mykchaylov, V. Shunko, and A. Yuslenko, "Uranium deposits associated with Na-metasomatism from central Ukraine: a review of some of the major deposits and genetic constraints," Ore Geol. Rev. **44**, 82–108 (2012).
69. M. Leisen, M.-Ch. Boiron, A. Richard, and J. Dubessy, "Determination of Cl and Br concentrations in individual fluid inclusions by combining microthermometry and LA-ICP MS analysis: implications for the origin of salinity in crustal fluids," Chem. Geol **330–331**, 197–206 (2012).
70. S. Staude, W. Werner, T. Mordhorst, K. Wemmer, D. E. Jacob, and G. Markl, "Multi-Stage Ag–Bi–Co–Ni–U and Cu–Bi Vein mineralization at Wittichen, Schwarzwald, SW Germany: geological setting, ore mineralogy, and fluid evolution," Miner. Deposita **47**, 251–276 (2012).
71. A. Richard, P. Boulvais, J. Mercadier, M.-C. Boiron, M. Cathelineau, M. Cuney, and C. France-Lanord, "From evaporated seawater to uranium-mineralizing brines: isotopic and trace element study of quartz–dolomite veins in the Athabasca system," Geochim. Cosmochim. Acta **113**, 38–59 (2013).
72. A. Richard, J. Cauzid, M. Cathelineau, M.-C. Boiron, J. Mercadier, and M. Cuney, "Synchrotron XRF and XANES investigation of uranium speciation and element distribution in fluid inclusions from unconformity-related uranium deposits," Geofluids **13**, 101–111 (2013).
73. G. B. Naumow and O. F. Mironowa, "Das Verhalten der Kohlensaure in Hydrothermalen Losungen bei der Bildung der Quarz–Nasturan–Kalzit Gange des Erzgebirges," Zeitschrift Angew. Geol. **15**, 240–241 (1969).
74. G. B. Naumov, O. F. Mironova, and M. B. Kuz'min, "Carbon dioxide of hydrothermal solutions," in Essays on Modern Geochemistry and Analytical Chemistry (Nauka, Moscow, 1972), pp. 166–172.
75. O. F. Mironova, V. B. Naumov, and A. N. Salazkin, "Study of gas–liquid inclusions with H_2S in quartz from the East Transbaikalia," Geokhimiya, No. 12, 1838–1845 (1973).
76. V. Yu. Prokof'ev, V. B. Naumov, O. F. Mironova, and N. T. Sokolova, "Study of fluid inclusions with high-density H_2S," Geokhimiya, No. 7, 948–953 (1990).
77. V. B. Naumov, V. I. Kovalenko, V. A. Dorofeeva, A. V. Girnis, and V. V. Yarmolyuk, "Average compositions of igneous melts from main geodynamic settings according to the investigation of melt inclusions in minerals and quenched glasses of rocks," Geochem. Int. **48** (12), 1185–1208 (2010).
78. I. A. Andreeva, V. I. Kovalenko, A. V. Nikiforov, and N. N. Kononkova, "Compositions of magmas, formation conditions, and genesis of carbonate-bearing ijolites and carbonatites of the Belaya Zima alkaline carbonatite complex, Eastern Sayan," Petrology **15** (6), 551–574 (2007).
79. M. Gaeta, T. Di Rocco, and C. Freda, "Carbonate assimilation in open magmatic systems: the role of melt-bearing skarns and cumulate-forming processes," J. Petrol. **50**, 361–385 (2009).
80. I. S. Peretyazhko, E. A. Tsareva, and V. E. Zagorskii, "Immiscibility of calcium fluoride and aluminosilicate melts in ongonite from the Ary-Bulak Intrusion, eastern Transbaikal Region," Dokl. Earth Sci. **413** (2), 315–320 (2007).
81. V. I. Kovalenko, G. M. Tsareva, R. L. Hervig, and V. V. Yarmolyuk, "Trace elements and water in melt inclusions (magmas) of rare-metal alkaline granites," Dokl. Ross. Akad. Nauk **326**, 349–353 (1992).
82. A. Audetat, "Source and evolution of molybdenum in the porphyry Mo(-Nb) deposit at Cave Peak, Texas," J. Petrol. **51**, 1739–1760 (2010).
83. I. A. Andreeva and V. I. Kovalenko, "Evolution of the trachydacite and pantellerite magmas of the bimodal volcanic association of Dzarta-Khuduk, central Mongolia: investigation of inclusions in minerals," Petrology **19** (4), 348–369 (2011).
84. T. R. Gray, J. J. Hanley, J. Dostal, and M. Guillong, "Magmatic enrichment of uranium, thorium, and rare earth elements in Late Paleozoic rhyolites of southern

New Brunswick, Canada: evidence from silicate melt inclusions," Econ. Geol. **106**, 127–143 (2011).

85. A. Richard, C. Rozsypal, J. Mercadier, D. A. Banks, M. Cuney, M. C. Boiron, and M. Cathelineau, "Giant uranium deposits formed from exceptionally uranium-rich acidic brines," Nature Geosci. **5**, 142–146 (2012).
86. G. Graser, J. Potter, J. Koehler, and G. Markl, "Isotope, major, minor and trace element geochemistry of late-magmatic fluids in the peralkaline Ilimaussaq Intrusion, South Greenland," Lithos **106**, 207–221 (2008).
87. E. Tomlinson, I. De Schriver, K. De Corte, A. P. Jones, L. Moens, and F. Vanhaecke, "Trace element compositions of submicroscopic inclusions in coated diamond: a tool for understanding diamond petrogenesis," Geochim. Cosmochim. Acta **69**, 4719–4732 (2005).
88. A. Y. Borisova, R. Thomas, S. Salvi, F. Candaudap, A. Lanzanova, and J. Chmeleff, "Tin and associated metal and metalloid geochemistry by femtosecond LA-ICP-QMS microanalysis of pegmatite–leucogranite melt and fluid inclusions: new evidence for melt–melt–fluid immiscibility," Mineral. Mag. **76**, 91–113 (2012).
89. A. Audetat and T. Pettke, "The magmatic-hydrothermal evolution of two barren granites: a melt and fluid inclusion study of the Rito del Medio and Canada Pinabete plutons in northern New Mexico (USA)," Geochim. Cosmochim. Acta **67**, 1348–1351 (2003).
90. M. Leisen, J. Dubessy, M.-C. Boiron, and P. Lach, "Improvement of the determination of element concentrations in quartz-hosted fluid inclusions by LA-ICP-MS and Pitzer thermodynamic modeling of ice melting temperature," Geochim. Cosmochim. Acta **90**, 110–125 (2012).
91. E. L. Tomlinson and W. Muller, "A snapshot of mantle metasomatism: trace element analysis of coexisting fluid (LA-ICP-MS) and silicate (SIMS) inclusions in fibrous diamonds," Earth Planet. Sci. Lett. **279**, 362–372 (2009).

Translated by E. Kurdyukov